FAILURE INITIATION AND EFFECT OF DEFECTS IN STRUCTURAL DISCONTINUOUS FIBER COMPOSITES

Bruno Boursier, Alfonso Lopez
Hexcel Research and Technology
1711 Dublin Blvd
Dublin, CA 94568

ABSTRACT

Discontinuous Fiber Composites (DFC) molded by compression molding are increasingly being used for structural parts of complex geometries. HexMC®, an advanced carbon/epoxy form of DFC produced by Hexcel, was used for this study. It is used for structural parts in the new generation of commercial airplanes. DFC do not behave structurally like Continuous Fiber Composites (CFC). These differences are driving the development of DFC specific design methods, material allowable and design values. Some of the definitions for failure initiation developed by the industry for CFC do not apply to DFC. Similarly, defects affecting CFC do not affect DFC in the same way. This paper reports and discusses some of the findings about the differences in failure initiation and effect of defects between DFC and CFC. The need for a new approach to non destructive testing, including pass/fail criteria are also discussed. Trial results using Acoustic Emission, a potential non destructive technique for DFC, are also presented.

1. INTRODUCTION

The new generation of commercial transport aircraft is using composite materials extensively. The structural elements of these new planes are very similar to their metal predecessors. Fuselages for example are assemblies of skins stringers, frames, window frames, etc. Such assemblies require a multitude of load carrying connector parts. These connector parts have complex geometries as well as load paths that make them difficult and expensive to produce with conventional aerospace established composite product forms and processes. These parts can be produced out of aluminum, but their weight and issues with fatigue and galvanic corrosion when in contact with carbon composite greatly lessen the benefits of making composite airplanes. Epoxy impregnated Discontinuous Fiber Composite (DFC) have the formability to mold such complex geometry parts by compression molding. DFC product forms such as sheet molding compound (SMC) or bulk molding compound (BMC) have long been used in industrial and automotive applications such as body panels, but not for structural parts as critical as these aircraft parts. Hexcel has developed a high performance form of DFC that has been used for structural applications in industrial and recreational markets for about 12 years [1].

Using DFC for structural applications in aerospace has revived an interest in better understanding the behavior of this type of materials from which better structural analysis methods can be developed. Since Hexcel HexMC is currently in production to make aerospace primary structure parts; it is a pathfinder for developing better understanding of DFC behavior from which testing, analysis and inspection methods can be developed. This work was done using aerospace grade HexMC made from Hexcel 8552/AS4 unidirectional tape (“UD”). It will

often be referred as “DFC” in this paper as most of the findings (in trend) are valid for DFC in general.

1.1 DFC Properties Overview

For high performance DFC, special attention is taken to produce a high level of orientation randomness of the short fibers, and to also maintain straight fibers . High performance DFC like HexMC also have high fiber volume (>50%) and fiber length greater than 25 mm. This guaranties fiber to fiber load paths. As a result, moduli of such high performance DFC are similar to a quasi-isotropic (QI) lay-up made from the same fiber and resin constituents, see Figure 1.

Part of the difference between DFC and QI laminates comes from the fact that DFC do not concentrate on the 0,+/-45, 90 directions as are QI lay-ups.

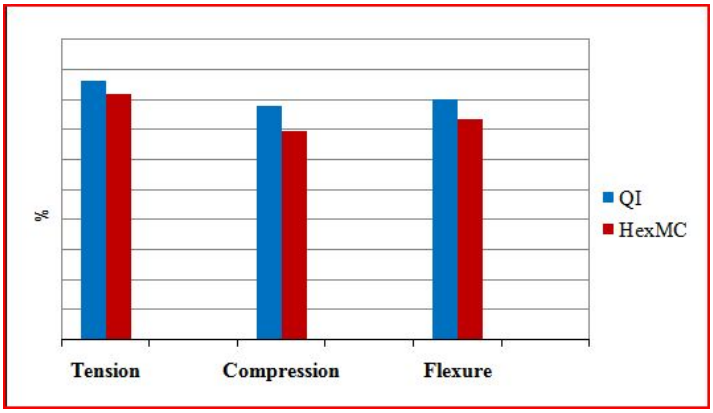

Figure 1. Comparison of tension, compression and flexure moduli of DFC (HexMC) and quasi isotropic laminate made from the same prepreg batch.

As a result, the coupon stiffness can be predicted fairly accurately by using properties from QI lay-up with the same fiber, resin and fiber volume as high performance DFC. If care is taken to maintain randomness of the DFC during the high pressure compression molding of parts then part stiffness can be estimated using QI properties. However, strengths of DFC do not follow the strengths of QI laminate, as shown in Figure 2.

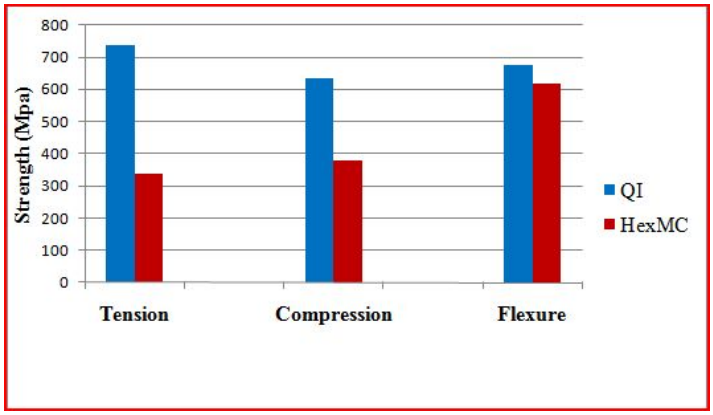

Figure 2. Comparison of tension, compression and flexure strength of DFC (HexMC) and quasi isotropic laminate made from the same prepreg batch

This difference in strengths between DFC and CFC is typical. The exact failure mechanism of DFC is more complex than for CFC, and there are no (industry accepted) failure criteria nor analysis methods to accurately predict ultimate strength of DFC parts. Work is on-going toward that goal at Hexcel as well as through an Advanced Materials for Transport Aircraft Structures). AMTAS is one of two university groups that together form the Joint Advanced Materials & Structures (JAMS) Center of Excellence. JAMS is supported by the FAA and several industrial partners [2].

1.2 Insensitivity to Holes and Defects

It was also found that DFCs are relatively non affected by notches/ holes especially when compared with CFC, see Figure 3.

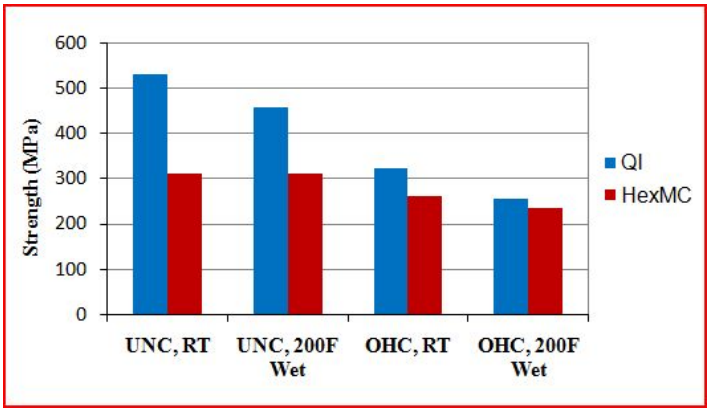

Figure 3. Compression strengths for un-notched and notched coupons and Compression after Impact (CAI) of DFC (HexMC) and quasi isotropic laminate (QI) made from the same prepreg batch. Coupons were 30.5cm long x 3.8cm wide, the hole was 6.35 mm diameter.

In addition to insensitivity of holes, HexMC was also found to be insensitive to defects during qualification and certification testing of over 1400 parts. Parts were tested in pristine conditions (no defects determined by ultrasonic testing), as well as with three types of defects:

1. Molded-in defects (1.27 cm x 1.27 cm brass covered with Teflon) imbedded between HexMC plies
2. Visible damage from impact
3. Incidental damage: cuts made with a saw and/or visible surface damages

These defects were located in high stress areas of the parts as determined by structural analysis and verified by testing of the pristine parts. Parts always had a combination of defects and damage. All parts were tested statically and many were also tested in fatigue depending on the application. The fatigue cycle typically represented the service load for three times the design life of the airplane. All parts survived the fatigue testing and were subsequently tested to failure in static. The failure load of these parts after fatigue was the same as non- fatigued parts. Even fatigued parts with defects had the same static strength as pristine parts that had not been submitted to fatigue.

Figure 4 shows typical results from a series of tests on pristine parts and parts with molded-in defects and that were also damaged.

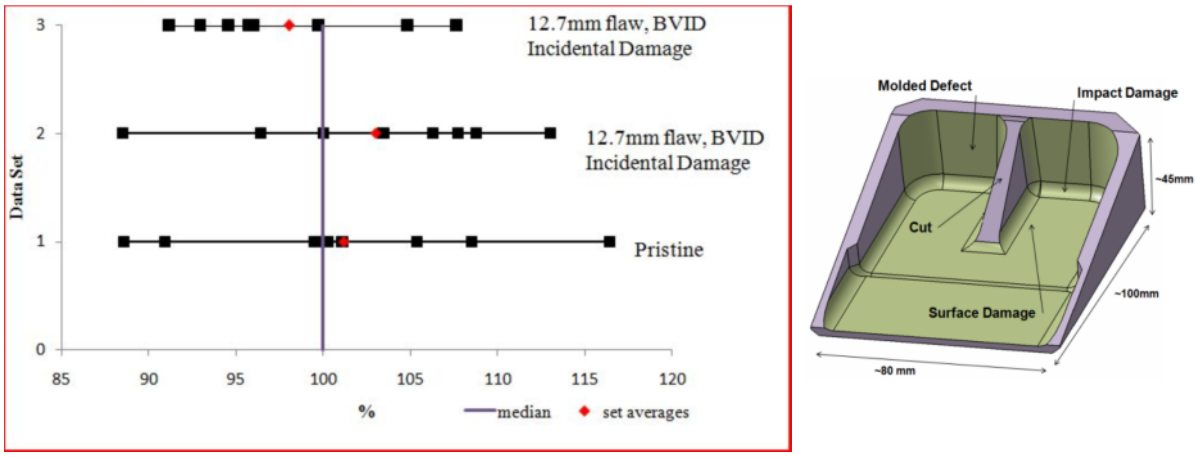

Figure 4. Example of static test results for three sets of parts with and without defects.

Even with substantial defects and damages, this complex 3D part had no loss of part strength. Each square dot represents a test. Statistical analysis shows all the results fall within the same population. Further, the impact “footprint” as detected by ultrasonic testing was found to be smaller for DFC than for CFC (QI laminate of same thickness).

Conversely, when parts are produced with a Quasi Isotropic lay-up of the same batches of 8552/AS4 UD used to make DFC parts, sensitivity of Barely Visible Impact Damages (BVID) reappears. An example is shown in Figure 5 and Figure 6.

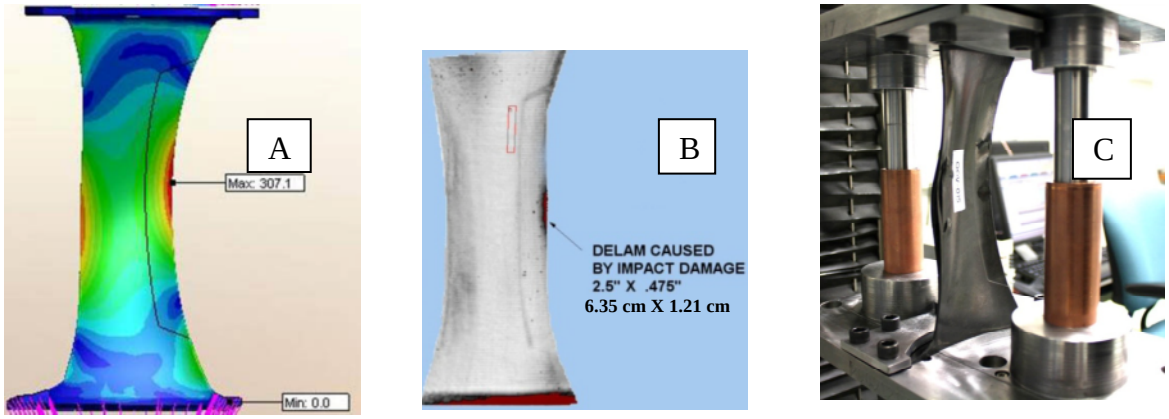

Figure 5. Complex part made with DFC and CFC. A) FEA stress analysis predicting high stress areas. B) NDI of impact damage in the predicted highest stress area. C) Compression testing showing failure at the predicted location.

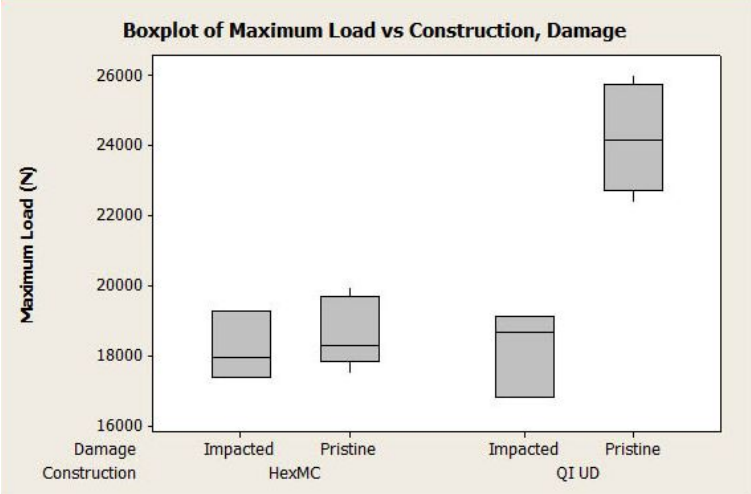

Figure 6. Test results for HexMC parts and Quasi Isotropic UD (QI UD) parts shown in figure 5.

All these results and observations indicate that the failure mechanisms in DFC are not the same as for CFC. The failure initiation might be the same for both material forms, DFC might even be more prone to start cracks, but the failure propagation is very different. The random and entangled short fibers (5 cm) in HexMC appear to stop or at least greatly slow crack propagation.

In CFC, cracks propagate more easily between plies resultant in the “first ply failure”. Hence crack initiation is often defined as failure, at least for structural aerospace applications. During coupon or part testing, this event is recorded as either an abrupt drop of load, change in strain or even an audible sound.

Upon loading a DFC part/coupon, audible pings and tings emanate much earlier than in CFC laminates. Such noises are the telltale of cracking and first ply failure in CFC. Understandably, there has been concerns about this with DFC. Hence, we set out to investigate the relation of the first cracks/sounds to the ultimate tensile strength of the material. As we found out, the stress

level at the first crack/sound gave no indication of ultimate properties. The location of the first cracks did not predict the failure location either. We further demonstrated that cracks resulting from pre-loading and/or fatiguing of coupons were not detrimental to the ultimate properties.

2. EXPERIMENTATION

Given the association of first ply failure in classic CFC with their ultimate strength, it was of interest to investigate the same link for DFC. Both the static tensile and fatigue behaviors of HexMC were investigated.

- Test samples: Tensile samples were cut from 33 cm by 33 cm compression molded HexMC panels
    - HexMC: 8552/AS4/38% Resin Content, 1900 gram per square meter nominal
    - Laminate: 3 plies of HexMC, nominal laminate thickness 3.0 mm (0.12")
    - Processing: compression molding
    - Tensile sample preparation: use a diamond grit wet abrasion saw
        - Trim 12.7 mm (0.5 in) from the molding panel edge
        - Cut specimens 3.17 cm (1.25 in) or 3.81 cm (1.5 in) wide.
- Crack location: the location of the first crack(s) was identified using acoustic emission monitoring and examined to understand where cracks are likely to start.
    - Crack location using Euro Physical Acoustics system MISTRAS – 4.
        - Number of sensors - 2
        - Resonant frequency (kHz) 300
        - Data acquisition filter (kHz) 100 - 1200
        - Preamplifier type 2/4/6 Gain (dB) : 40
        - Preamplifier filter (kHz) 20 - 1200
        - Acquisition threshold 35 dBEA (dBEA : m*volt/sensor output*)
    - Liquid penetrant was used to find surface cracks at AE signal locations (Sherwin Double Check DP-50 red penetrant and D-100 developer).
    - Light microscopy was used to examine cracks.
- Effect of the first crack on ultimate strength: The first audible crack event was recorded electronically while the static strength of a control set of specimens was measured.
        - 12 coupons were tested according to ASTM3039
        - 12 were tested in a step wise load cycle. Load and unload, to zero strain, at 10% increments until failure (10%, 20%, 30%, etc..)
    - Monitored crack occurrence by acoustic emission. Different sample set.
        - DECI SE150-M or Score Atlanta SE150-M transducer with 150 KHz resonant frequency output, 0 to 10 volt signal output
        - Vellen Acoustic Emission Preamp model AEP4, 34 dB gain, 2.5 KHz-3MHz
        - Data acquisition at 500KHz with RMS averaging at 10 millisecond periods. National instruments hardware and Lab View software for data acquisition.
- Ultimate strength after fatigue loading: ultimate strength of HexMC specimens was measured after loading samples in tensile-tensile fatigue per the procedure below:

- Overload - one cycle at 66% of expected ultimate strength
- Low Cycle Fatigue: 110 cycles at 60% of expected ultimate strength, 1 Hz, R=0.1
- High Cycle Fatigue: 10^6 cycles at 42% of expected ultimate strength, 5 Hz, R=0.1

3. RESULTS

3.1 Inspection of First Cracks

The objective for observing the first crack(s) was to understand where they occur, and why they don't necessarily affect the ultimate strength of the sample. Even the location of the first crack is not necessarily a telltale marker of where the specimen would fail. Figure 7 shows an example of four specimens checked for cracks before being tested to ultimate failure.

To understand why DFC has early cracking, we inspected six tensile samples after they were loaded to the first audible sound.

Our visual observations of first cracks show they generally occur at the surface and appear in chips that are off-axis to the load direction, or, at the interface between surface chips where there is a resin rich boundary layer (either at the ends or at the side interface). Cracking beyond the first few surface chips depends on the local chip orientation. Where cracks are more prevalent in areas where chips are not well aligned with the test direction.

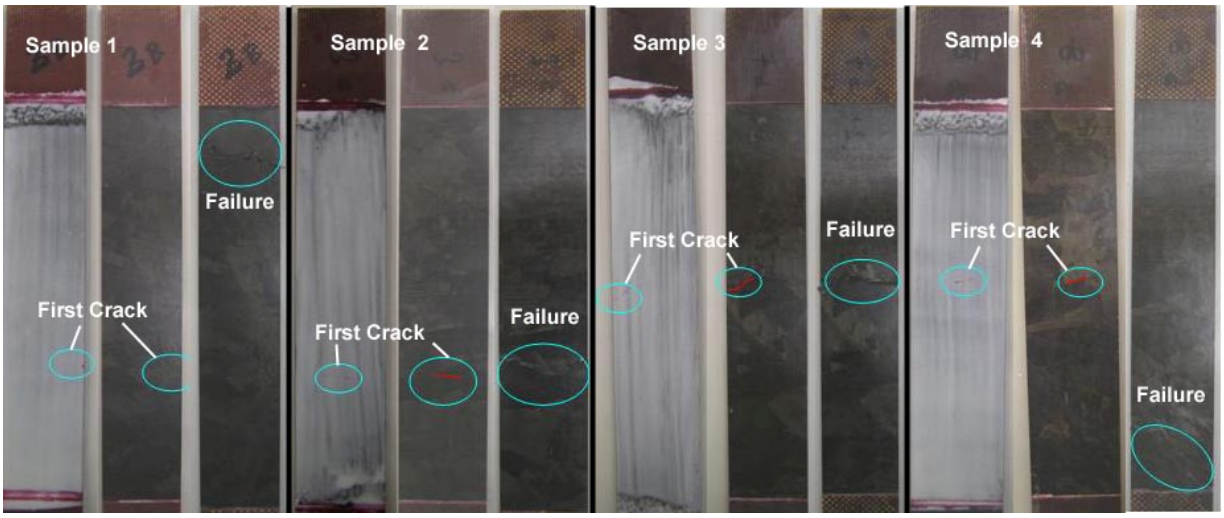

Figure 7. HexMC tensile test samples checked for surface cracks after the first audible crack was heard. Subsequent failure was not necessarily at the crack location indicated.

From six tensile samples loaded to the first audible crack sound, we found surface cracks on four of them. We could not find surface or interior cracks on the other two. Crack locations were detected via two methods. Acoustic emission was used to locate crack events and liquid penetrant was used to detect surface cracks (see the test plan for AE set up). Figure 8 shows pictures of the test samples after loading. "LP" notations denote surface cracks detected with liquid penetrant. If no cracks were detected using liquid penetrant, a horizontal line indicates the located acoustic signal. In the later case the sample was cut along the "A" line and inspected.

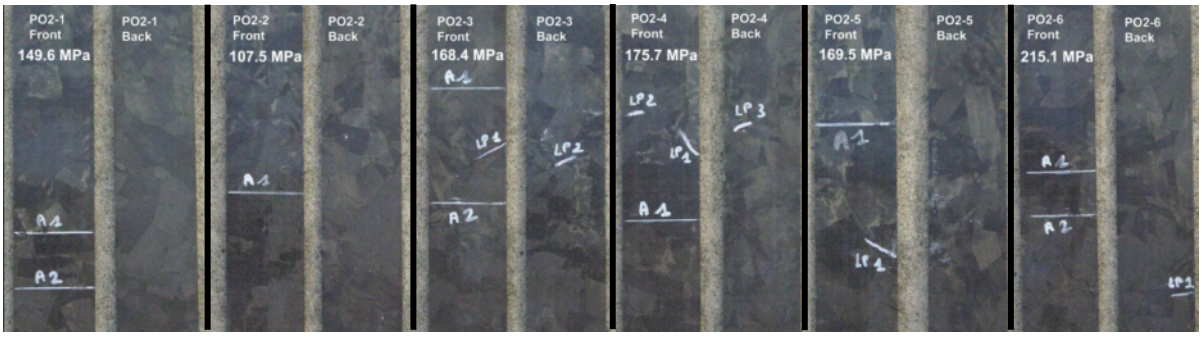

Figure 8. Pictures for tensile samples used to inspect the first cracks. “LP” notation denotes cracks detected by acoustic emission and liquid penetrant. “A” denotes locations where acoustic emission was detected, but liquid penetrant did not reveal surface cracks. Noted are the identification and first sound loading for each sample.

Out of the four specimens with verified surface cracks, only one had cracking beyond the first few chip layers (PO2-6 LP1). Figure 9 shows the micrograph for this sample. In this case, the sample was loaded to 213 MPa (31 ksi), higher than any other sample, and several chips at this location were angled more than 45 degrees from the load direction.

No interior cracks could be found at locations with AE signals only. It is possible the cracks were cut through and destroyed, the marked locations were slightly off, or crack sizes were so small they were not noticed. Table 1 summarizes the average chip angle at LP locations.

Table 1. Chip angles at LP surface cracks. Angles are given relative to the load direction, complementary angles are not differentiated. Angles were calculated visually based on the length of the major and minor fiber axis.

		chip angle (degrees)				
sample	location	surface chip	chip 2	chip 3	chip 4	crack comment
PO2-3	LP1	62.8	48.7	56.8	48.0	at chip edge
PO2-3	LP2	20.8	68.7	44.4	56.7	at chip edge
PO2-4	LP1	69.9	31.3	17.8	39.0	void initiator at chip edge
PO2-4	LP2	71.0	5.9	5.3	16.7	at chip edge
PO2-4	LP3	22.9	51.7	68.8	17.2	at chip end
PO2-5	LP1	46.0	38.4	55.1	68.7	void initiator
PO2-6	LP1	71.7	42.5	48.7	63.9	within chip

For crack locations with shallow angled surface chips, it was verified that cracks initiated directly at chip end/edge. Figure 10 shows micrographs for samples PO2-3 LP2 and PO2-4 LP3. Both locations show cracks initiating directly at a chip interface, where there is a resin rich area. Some cracks initiated as a result of preexisting surface defect. Figure 11 shows a micrograph for crack PO2-4 LP1, which started from a surface void.

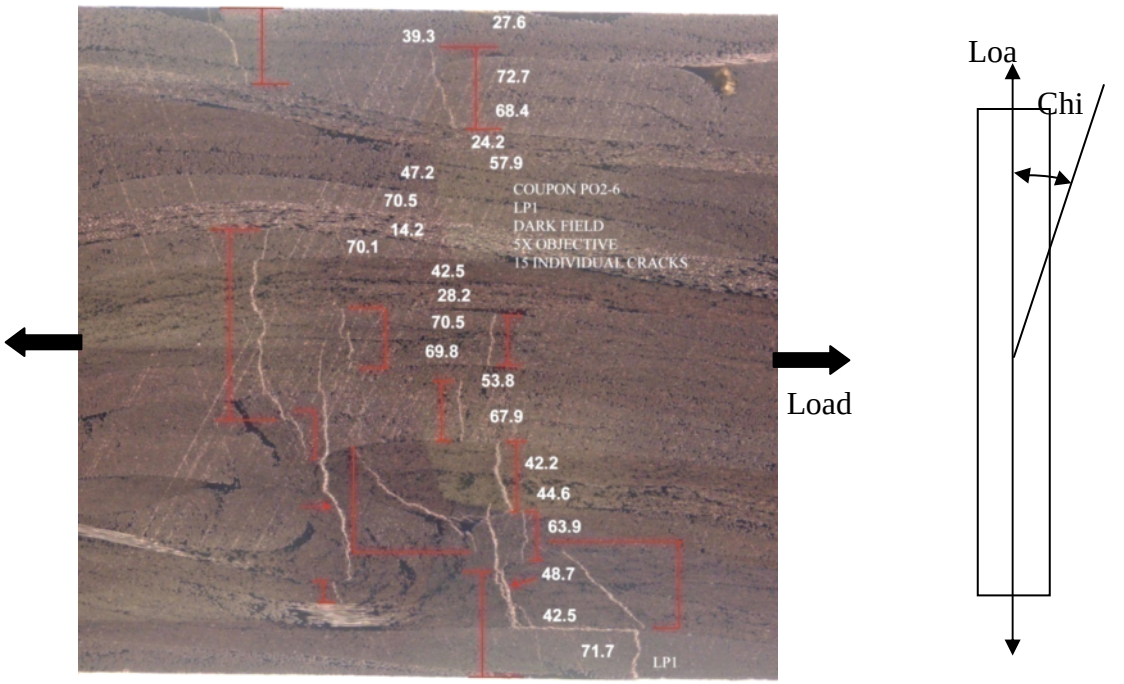

Figure 9. This sample had cracking beyond the first few surface chips. Noted on each chip is the fiber angle relative to the loading direction. Most chips are aligned more than 45 degrees from the load.

Given the visual observations, it is reasonable to conclude first cracks occur at the surface since:

- The surface can have pin holes, resin pockets or other small defect from molding. These can be locations for first crack initiation.
- The surface chips only have shear reinforcement on one side. Thus tensile forces at the chip ends and edges will be slightly higher (consider a single lap joint compared to a double lap joint).
- The edges of a sample are more prone to early cracks since they are cut. This can induces microscopic defects, which are crack initiators, most cracks inspected were at the edge, see Figure 8., We also inspected fatigue parts, which showed multiple cracks at the edges. See section 3.3.

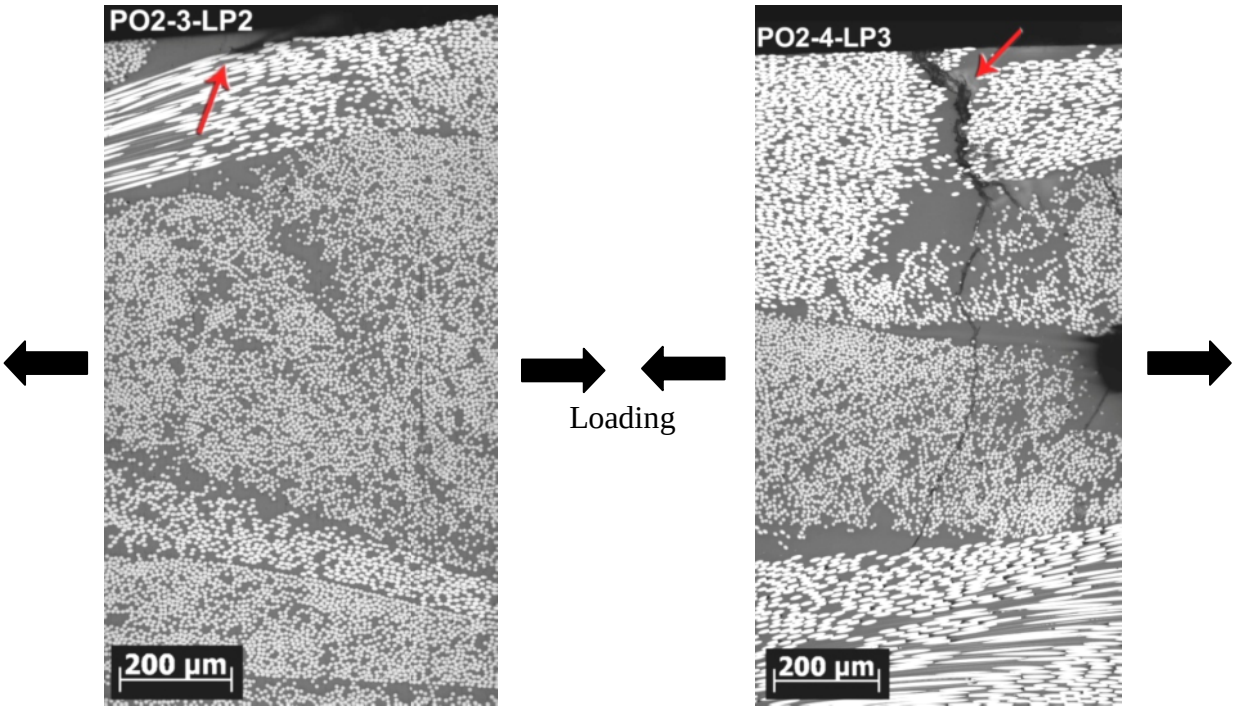

Figure 10. Micrographs of two crack locations showing initiation at the chip end. The surface chips are well aligned to the load direction. The crack at PO2-3-LP2 is a shallow surface crack. The crack at PO2-4-LP3 formed between chip ends and propagated through chips at an off angle from the load direction.

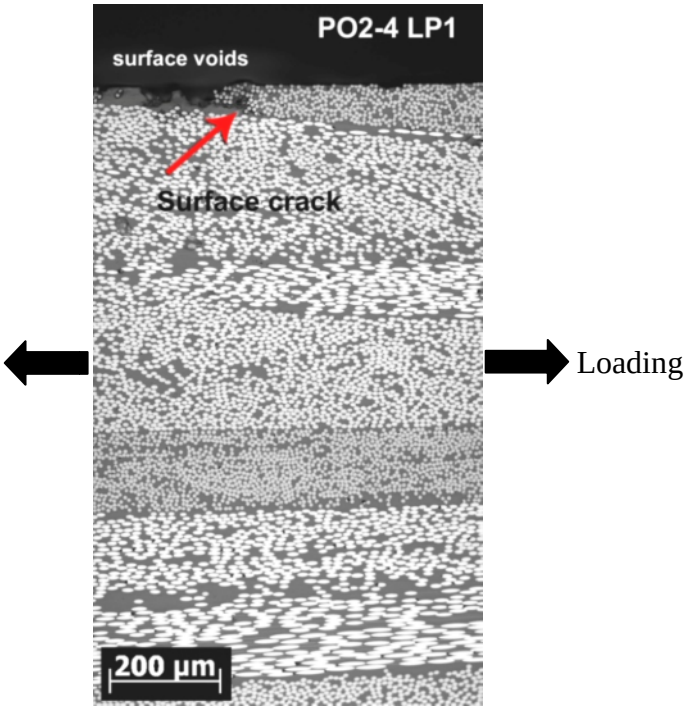

Figure 11. Micrograph showing a shallow surface crack. The crack likely started at the surface voids.

3.2 Relation of First Crack to Static Tensile Strength

The stress level at which the first audible crack occurs in DFC is not an accurate predictor of ultimate properties, unlike a first ply failure in CFC. We tested 24 HexMC specimens (ten samples from two separate panels, and four samples from a third panel) in static or step wise load cycling. 12 specimens were tested following ASTM 3039. Another 12 specimens were step cycled to monitor modulus changes due to increasing level of cracks; see the test plan in the Experimentation section.

For a given panel, the average tensile strength from statically tested specimens was used as the expected strength for step cycled specimens. An event button was used to record the first crack heard for both static and step cycled specimen. Figure 12 shows a scatter plot of all results. Statistically, there is not a correlation between the stress when the first audible crack occurs and the ultimate stress of the sample. The data has a Pearson correlation strength of 0.362 and P-value of 0.082. Many of the samples with high ultimate strength exhibited the first audible cracks later than lower strength specimens, but it was not consistently the case. At best, there is a wide envelope in which the first audible crack could indicate the ultimate strength level. Later on, we explored the failure envelope for samples monitored with acoustic emission.

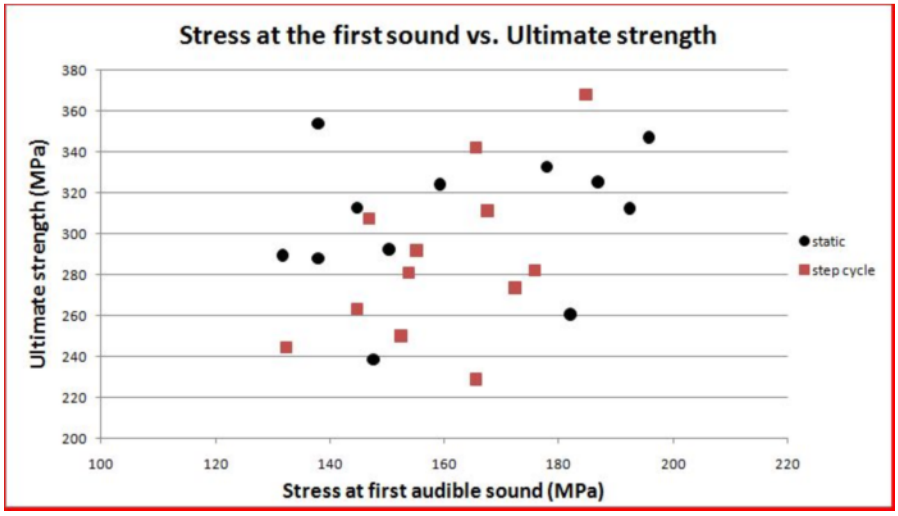

Figure 12. Scatter plot showing the ultimate strength in relation to the stress when the first sound occurred. Each samples was 3.17 cm wide, average thickness of 0.338 cm and 56.5% fiber volume. Overall correlation: Pearson correlation strength 0.362, P-value 0.082. Static samples correlation: Pearson correlation strength 0.263, P-value 0.408. Step Cycled sample correlation: Pearson correlation strength 0.530, and P-value 0.077

Since detecting audible cracks is operator subjective, we also monitored 75 tensile specimens using an acoustic emission transducer. Specimens were 3.81 cm wide with a nominal thickness of 3 mm. Acquisition parameters were 500 KHz rate with RMS averaging over a 10 millisecond period. Since many first cracks were observed to form in areas with local chip misalignment to the load direction; it stands to reason samples with higher levels of chip misalignment should have cracks form at earlier load levels, and thus generate a detectable sound. We tested eight control specimens and specimens with deliberate defects to simulate off-axis chip concentrations. Samples with defects included:

- Varying levels of chip misalignment
    - 4 chips (surface chips or interply dispersed)
    - 8 chips (surface chips or interply dispersed)
    - 16 chips(surface chips or interply dispersed)
- Butt splice (cut the surface ply or center ply before molding)

Using acoustic emission for monitoring damage and predicting ultimate failure based on the AE signature levels is accepted for high pressure tanks, crane arms and wind blades [3][4][5]. This NDI monitoring method has gained more widespread use for CFC [6][7][8]. Hence, it is well suited for recording first cracks in DFC to see if they correlate to ultimate strength.

To compare the auditory first crack results with AE, we established a limit of 3.0 volts as the "auditory" threshold for AE monitoring. Crack events with an intensity of about 3.0 V seemed to be on the low end of being audible. As a reference, total failure crack events registered around 6.5V. (Figure 13 shows an example AE profile for a HexMC tensile sample). There was again no correlation between the first crack event and the ultimate strength, see Figure 14. While the average strength of samples with misalignment or butt splice defects went down, the stress at which point the first crack occurred did not change. This simply indicates first cracks in DFC occurred in areas with the weakest conformation; be it man-made or random.

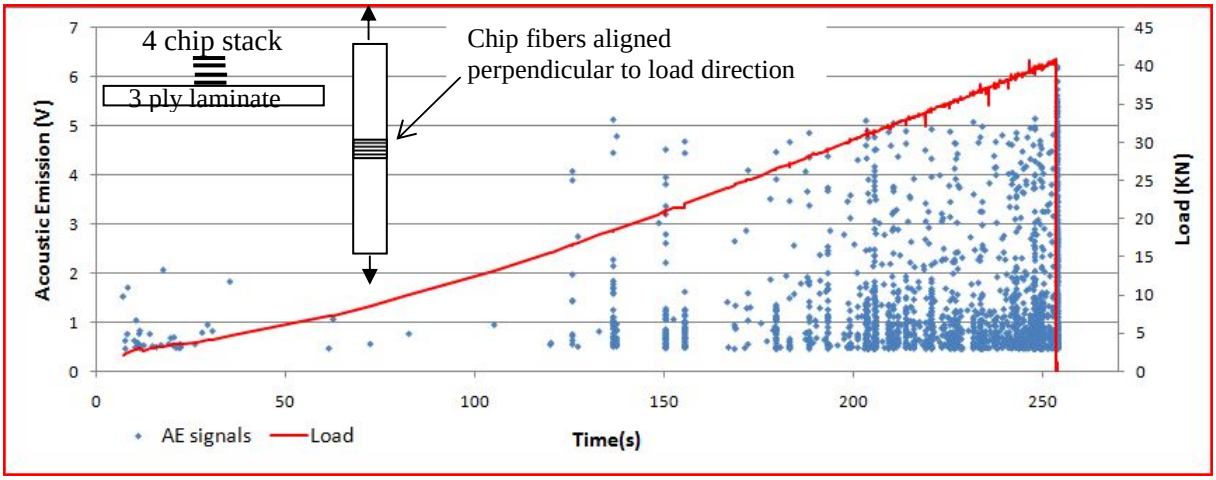

Figure 13. Example AE profile for a HexMC tensile test. This sample had four chips manually oriented and stacked perpendicular to the load direction which represented about 16% of the total number of stacked chips through the thickness (≅ 24 chips). This sample failed at 343 MPa - 106% of the nominal strength (324 MPa).

Table 2 summarizes the average strength results for each category of specimens. Expectedly, samples with deliberate defects generally fail at a lower load. However, the stress at which the first AE peak occurs stays the same. For specimens with no defects, the average stress at the first AE peak was 146 ±34 MPa, while samples with a butt splice in them had the first AE peak around 122 ±28 MPa.

Table 2. Average results of monitoring the first AE peak over 3V. 324.1 MPa was set as the nominal strength. As defect severity increases strength decreases, but the stress at the first crack detected does not change significantly.

Panel ID	Defect location	Defect type	Number of samples	Strength (MPa)	Strength SD (MPa)	Stress at first peak (MPa)	Stress at first peak SD (MPa)
IR999	no defect	no defect	8	313.1	29.3	146.30	33.84
IR926-IR974	surface	4 chip	11	289.2	49.2	132.11	29.67
IR987	distributed	4 chip	6	228.5	67.0	137.10	22.19
IR926-IR971	surface	8 chip	12	283.9	51.4	128.53	45.23
IR988	distributed	8 chip	7	290.4	17.2	133.54	21.82
IR925-IR972	surface	16 chip	12	247.7	28.2	176.74	24.51
IR925-IR973	surface	butt splice	12	197.1	21.3	112.52	23.69
IR989	center	butt splice	7	211.2	32.4	132.66	33.84

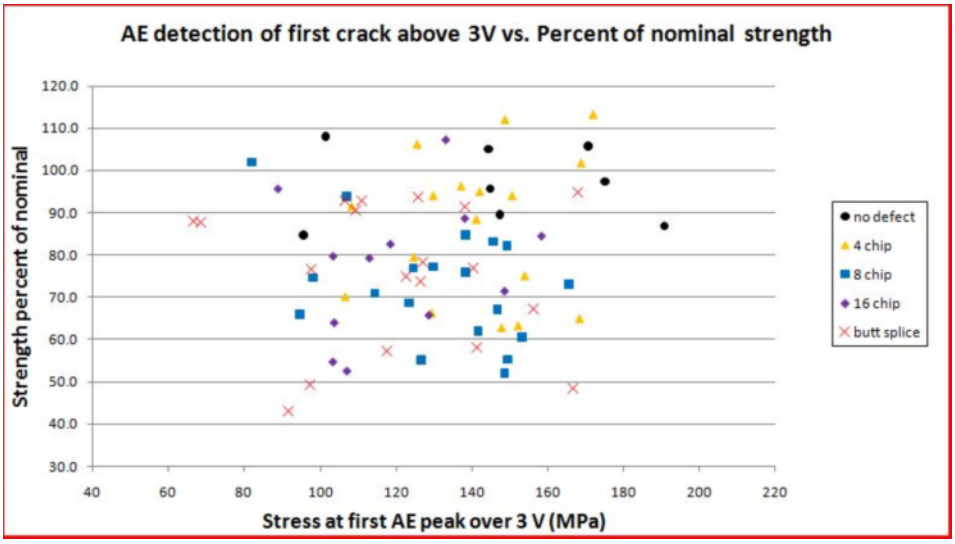

Figure 14. Scatter plot of static tensile samples monitored with an AE transducer. The y axis is based on a nominal strength of 324 MPa . Each samples was 38 mm wide and 3.0 mm nominal thickness. Overall correlation: Pearson correlation strength 0.087, P-value of 0.457.

3.3 Effect of First Cracks on Fatigue Life

We showed the stress level at which the first audible crack occurs did not serve to accurately gauge the ultimate strength. The same was true in fatigue. Even after 10^6 fatigue cycles, the average ultimate tensile strength did not change.

To test if fatigue cracking had an effect on the ultimate strength in DFC, we ran 11 tensile-tensile fatigue experiments on specimens subjected to a 66% overload cycle followed by fatigue cycling at 60% and 42% of the expected ultimate stress, see the Experimentation section. The fatigue load cycle was based on static tensile testing of four specimens from each of two panels. Each panel had its own baseline strength calculated from these four specimens.

Figure 15 shows the baseline and fatigue results. As can be seen, the fatigued samples had no difference in terms of ultimate strength compared to their baseline. Some samples even had unintentional pre-existing surface defects, see Figure 16 C-scan.

Figure 16None of these samples had low strength. To further establish the degree of damage in the samples after fatigue, IR863 samples were inspected with liquid penetrant.

Figure 17 shows a hand sketch of surface cracks identified with liquid penetrant.

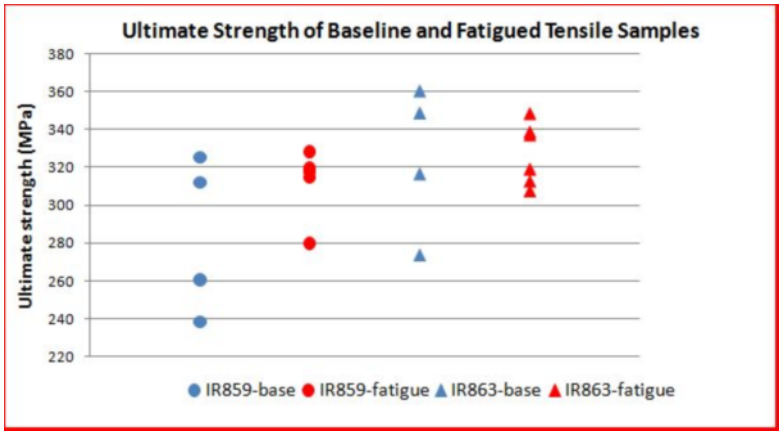

Figure 15. Plot for individual baseline and fatigue specimens showing no change in strength of fatigued coupons. See the experimental section for fatigue cycling definition.

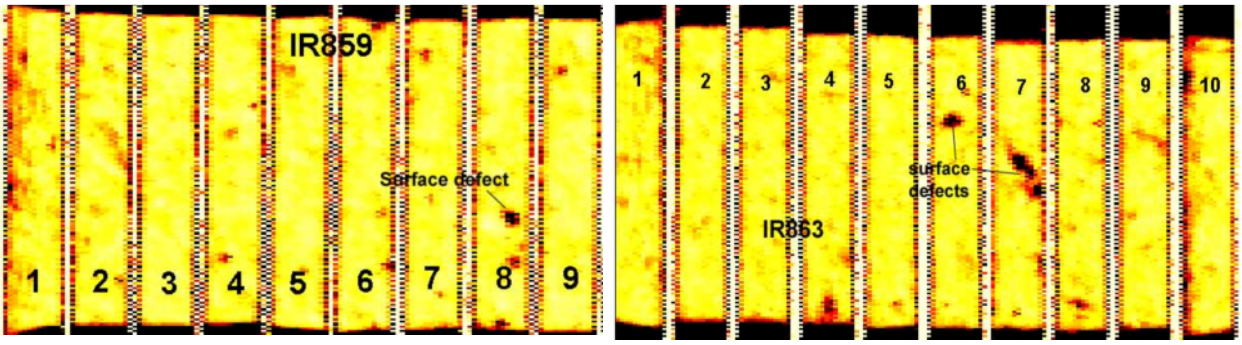

Figure 16. C-scans of HexMC samples for fatigue testing. Black areas indicate signal attenuation of more than 60%, reddish areas attenuation between 25% and less than 60%, yellow areas attenuation less than 25%.

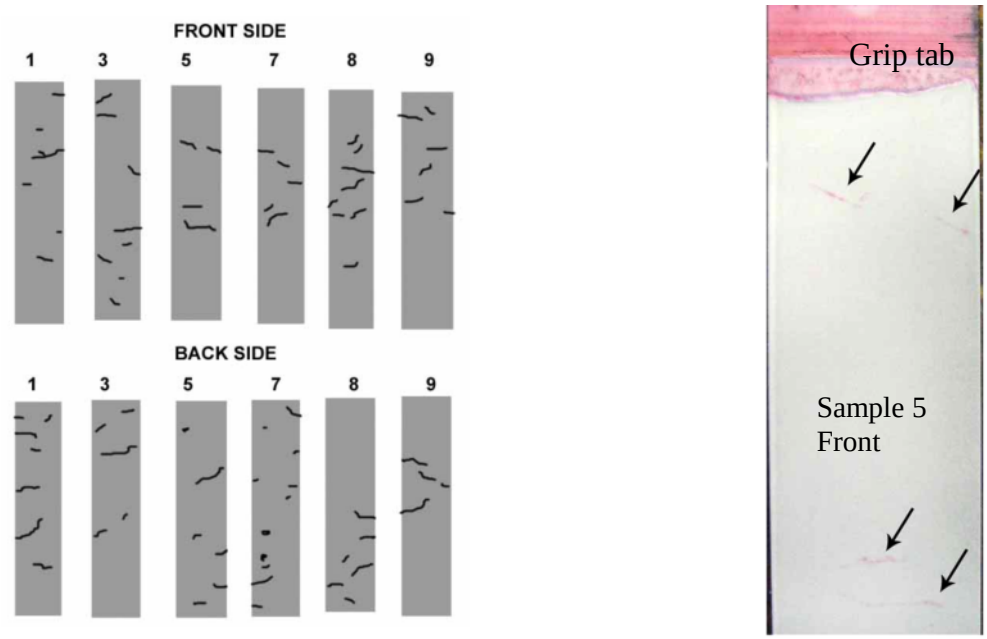

Figure 17. Sketch showing crack locations for fatigue set IR863. Liquid penetrant was used to identify surface cracks. The picture shows an example of how cracks appeared on a specimen

4. SUMMARY

HexMC, an advanced form of Discontinuous Fiber Composite (DFC), has proven to be an effective and robust material form to produce smaller-complex structural parts using advanced compression molding techniques. It is leading the way for DFC material forms to be used in more aerospace structural applications. However, using CFC structural analysis methods and failure criteria on DFC result in overdesigned parts. Additionally, using CFC non destructive inspection techniques and rejection criteria results in lower production yield. Developing a better understanding of the failure mechanism in DFC will greatly contribute to lower part weight and rejection rate, therefore lowering the cost of parts too.

This paper highlights differences found between HexMC and its quasi isotropic CFC counterpart. These findings are some of the building blocks needed to develop more adapted failure criteria and inspection techniques for DFC. Some of the key conclusions are:

- HexMC is relatively insensitive to holes compared to CFC
- HexMC is relatively insensitive to the types and sizes of defects that affect CFC
- HexMC is much more damage tolerant than CFC
- Initial cracks created while testing HexMC coupons/parts do not correlate to the ultimate failure load or give a good indication of the final failure location.
- HexMC is very tolerant to fatigue when compared to CFC.

In addition, acoustic emission was shown to be a useful method of monitoring real time crack damage. It could be used to aid inspecting DFC parts, but a more extensive study is needed to establish a robust inspection method and acceptance criteria.

5. REFERENCES

1. B. Boursier. “New possibilities with HexMC, a high performance moulding compound” , 22nd SAMPE European conference, March 2001
2. For more information about AMTAS-JAMS see http://depts.washington.edu/amtas/ and look for the project titled: “*Simplifying Certification of Discontinous Composite Material Forms for Primary Aircraft Structures” under Research - Active Projects (as of 2010)* - . http://depts.washington.edu/amtas/research/index.html#UW001. (accessed June 6, 2010).
3. ASTM International. Standard Practice for Determining Damage-Based Design Stress for Fiberglass Reinforced Plastic (FRP) Materials Using Acoustic Emission. ASTM International, 2008.
4. ASTM international. Standard Practice for Examination of Gas-Filled Filament-Wound Composite Pressure Vessels Using Acoustic Emission. ASTM International, 2008.
5. Paquette, J.A., and P.S. Veers. "Increased Strength in Wind Turbine Blades through Innovative Structural Design." Houston TX: AWEA Wind Power conference, 2008.
6. G., Caprino, and Teti R. "Quantitative Acoustic Emission for Fracture Behavior of Center-Hole GFRP Laminates." *Journal of Composite Materials* 28, no. 13 (1994).
7. G., Kamala, Hashemi J., and Barhorst A.A. "Discrete-Wavelet Analysis of Acoustic Emissions During Fatigue Loading of Carbon Fiber Reinforced Composites." *Journal of Reinforced Plastics and Composites* 20, no. 3 (2001).
8. L., Ndiaye, Maslouhi L., and Denault J. "Characterization of interfacial properties of composite materials by acoustic emission." *Polymer Composites* 21, no. 4 (2004).